Chem Soc Rev

TUTORIAL REVIEW

View Article Online
View Journal | View Issue

Cite this: *Chem. Soc. Rev.*, 2016, 45, 1794

Development of deep subsurface Raman spectroscopy for medical diagnosis and disease monitoring

Pavel Matousek*[a] and Nicholas Stone*[b]

Received 15th June 2015

DOI: 10.1039/c5cs00466g

www.rsc.org/chemsocrev

The recently developed array of Raman spectroscopy techniques for deep subsurface analysis of biological tissues unlocks new prospects for medical diagnosis and monitoring of various biological conditions. The central pillars of these methods comprise spatially offset Raman spectroscopy (SORS) and Transmission Raman Spectroscopy facilitating penetration depths into tissue up to two orders of magnitude greater than those achievable with conventional Raman spectroscopy. This article reviews these concepts and discusses their emerging medical applications including non-invasive breast cancer diagnosis, cancer margin evaluation, bone disorder detection and glucose level determination.

Key learning points
(1) Principle and context of deep Raman methods
(2) The capability and limitations of deep Raman methods
(3) Applicability areas of deep Raman methods in medical diagnosis and disease monitoring exemplified on real cases

Introduction

The recent advent of deep Raman spectroscopy techniques for subsurface analysis of biological tissues and other turbid media has opened new vistas in biomedical fields. These include non-invasive diagnosis of medical conditions and the monitoring of the presence and quantity of bio-analytes through skin. This can be performed at depths to several millimetres and in some cases several centimetres in biological samples. This is up to two orders of magnitude deeper than possible with conventional Raman spectroscopy approaches.

The cornerstones of these methods are Spatially Offset Raman Spectroscopy (SORS)[1] and Transmission Raman Spectroscopy (TRS).[2] The methods utilise the properties of photon diffusion in diffusely scattering (turbid) media in analogy with NIR absorption and fluorescence tomography techniques.[3] However with Raman spectroscopy much higher chemical specificity is available and this opens a host of new applications. These advances in Raman approaches stem from earlier research into temporal properties of migrating laser and Raman photons in turbid media using time-gated methods.[4] Although the time gated approaches are beneficial in subsurface probing in a number of situations their general applicability is hampered by the requirement for higher instrumental complexity and cost. Their medical use for *in vivo* applications is further restricted by safety laser intensity limits that are considerably more stringent with short pulsed laser beams than with continuous wave laser beams and penetration depths reached in biological tissues have not been as high as those accessible with SORS. For this reason we limit our review to methods utilising only continuous wave laser beams.

Deep Raman spectroscopy techniques

Spatially offset Raman spectroscopy – SORS

The SORS approach relies on spatially separating the collection Raman zone from the laser illumination zone on sample surface (see Fig. 1). A key benefit in realising these advances is the suppression of, often, intense interfering Raman and fluorescence contributions from the surface of sample which typically overwhelm much weaker signals from deeper zones in conventional backscattered Raman spectroscopy. Their suppression facilitates deeper probing within diffusely scattering media. The spatially offset Raman spectra contain varying relative contributions from

[a] *Central Laser Facility, Research Complex at Harwell, STFC Rutherford Appleton Laboratory, Harwell Oxford, OX11 0QX, UK. E-mail: Pavel.Matousek@stfc.ac.uk*
[b] *School of Physics, University of Exeter, Exeter EX4 4QL, UK. E-mail: N.Stone@exeter.ac.uk*

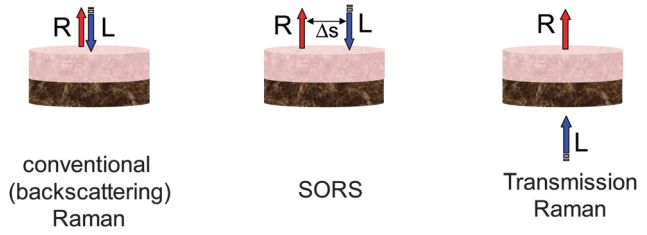

Fig. 1 Schematic diagrams of basic Raman spectroscopy modalities: conventional backscattering Raman, SORS and Raman transmission geometries. Legend: R – Raman light, L – laser beam, Δs – spatial offset.

different sample depths. This is consequence of the photons migrating to spatially separated zones near the surface having a higher likelihood of being lost at the sample-to-air interface than photons migrating through deeper zones. Statistically the mean photon penetration depth increases with increasing spatial offset Δs.

The deployment of SORS enables the retrieval of Raman spectra of sublayers within stratified turbid matrixes. For a two layer sample at least two SORS spectra acquired at different spatial offsets are required to recover the Raman spectra of individual layers. One such spectrum would typically be a zero spatially offset spectrum (equivalent to a conventional backscattering Raman spectrum) and one obtained at a non-zero spatial offset. The numerical recovery of spectra from individual layers is achieved by a scaled subtraction of the two spectra from each other with the multiplication factor adjusted to just cancel the contribution of the undesired layer leaving behind only the contributions from the layer one is recovering.[1] For a multilayer sample with n-layers one needs at least n-SORS spectra acquired at different spatial offsets to retrieve individual layer contributions, in analogy with solving linear equations with n-unknowns. Alternatively, an order of magnitude larger number of SORS spectra at different spatial offsets ($\geq 20n$) can be acquired and used in conjunction with multivariate methods such as band targeted entropy minimization (BTEM)[5] to retrieve the individual layer contributions. This approach could also be applicable to samples with an unknown number of layers. Other decomposition method have also been demonstrated such as an over-constrained extraction algorithm based on fitting with spectral libraries,[6] 2D correlation analysis.[7] There are other multivariate analysis methods that can also be potentially applicable. The reader can find their general description in ref. 8. It should be noted that the Raman signature of individual layers is recovered with no prior knowledge of the composition of any of the layers. In other words the data recovery is performed blind. As such the above processing steps are also amenable to automated data analysis. Apart from analysing effectively layers in tissue the SORS concept can also recover the chemical composition of other zones within tissue of arbitrary shape which are chemically distinct from its surroundings although in its basic form SORS would not provide information on the spatial properties and location of these zones.

With medical samples one would typically use laser excitation wavelengths within the NIR optical window of tissue (*e.g.* 785 or 830 nm). The optical window is a term often used for a spectral region where tissue is relatively transparent for light and stretches approximately from 650 to 950 nm. Its lower edge is given by the absorption of blood and the higher end by the absorption of water and lipids.[9] This range also enables optimum detection systems (silicon based CCD's) to be used and

Pavel Matousek

Prof. Pavel Matousek has worked at the Rutherford Appleton Laboratory in the area of vibrational spectroscopy for over 24 years. He pioneered the concepts of Kerr gated Raman spectroscopy and Spatially Offset Raman Spectroscopy (SORS). Pavel published over 190 peer-reviewed articles and filed 10 patents. His honours include the premier Royal Academy of Engineering's 2014 MacRobert Award, 2009 Charles Mann Award and the 2002 & 2006 Meggers Awards. Pavel is a Fellow of the Royal Society of Chemistry, a Fellow of the Society for Applied Spectroscopy, a Senior Fellow of STFC, an honorary professor at the University College London and a founding Director of Cobalt Light Systems.

Nicholas Stone

Prof. Nicholas Stone holds the position of Professor of Biomedical Imaging and Biosensing and Head of Physics and Astronomy at the University of Exeter. He also holds Honorary Consultant Clinical Scientist positions at Gloucestershire Hospitals and Royal Devon and Exeter Hospital. Nick has worked to pioneer the field of novel optical diagnostics within the clinical environment, recently moving from the NHS, after almost 20 years of working closely at the clinical/academic/commercial interface to pull-through novel technologies to be used where they have most clinical need. He recently won the International ICORS Raman Award for Most Innovative Technological Development and the UK Chief Scientific Officer's National R&D Award for 2009. He has published over 170 peer reviewed papers and proceedings and is a founding Director of CLIRSPEC, the International Society for Clinical Application of infrared and Raman spectroscopy.

minimises contribution from interfering tissue fluorescence. The Raman signal is typically coupled through imaging optics into an optical fibre bundle and relayed onto a slit of a low *f*-number spectrograph with fibres re-arranged to match the linear shape of the slit for optimum coupling efficiency. Alternatively a free-space coupling (*i.e.* without the recourse to optical fibres) can also be utilised. The detection is typically accomplished using a cooled, high performance, deep depletion CCD camera.

A number of SORS variants have been demonstrated in recent years. These include using single point collection and point laser deposition or ring or other patterned illumination and/or collection arrangement. Among these the arrangement with a ring shaped laser illumination and collection within a central zone ('inverse SORS') merits a particular note in the context of medical applications.[10,11] This is because the laser radiation can be spread over an extended area of the ring enabling to deliver large powers into tissue in situations where laser intensities are restricted, such as in *in vivo* applications. The ring-shaped laser beam can be formed using a conical lens (axicon). The spatial offset can be varied, for example, by altering the axicon-to-sample distance which changes the radius of the illumination ring.

The applicability of SORS is challenging or impossible in situations where the sample is highly absorbing at the laser or Raman signal wavelengths as this reduces photon propagation distances and as such penetration depths. A high level of fluorescence can also potentially drown weaker Raman signals. Although fluorescence originating from a non-target layer, for example, from samples surface, can be effectively reduced by SORS as outlined above.

The optimum magnitude of spatial offset is either determined empirically by trial and error using actual samples or tissue phantoms or its value can be determined numerically, *e.g.* using Monte Carlo simulations. A balance needs to be struck between adequate penetration depth, which requires increased spatial offset and the strength of deep layer Raman signals which diminishes with spatial offset; the target being the highest possible value of signal-to-noise ratio of the recovered Raman spectrum from the desired sublayer. This issue was investigated by Maher and Berger[12] and Bloomfield *et al.*[13] The latter study also concluded that a longer acquisition time should be spent on collecting spectra from larger spatial offsets for retrieving the optimum signal to noise ratio spectrum from the sublayer in situations where the overall collection times are restricted, *e.g.* due to patient being able to stay still only over limited time.

Transmission Raman

Transmission Raman spectroscopy was demonstrated in the early days of Raman spectroscopy,[14] however, its benefits for the non-invasive probing biological and pharmaceutical samples have only been recognised in full very recently. The technique can be considered a special case of SORS, where the laser beam and the Raman collection zone are separated to the extreme, being on the opposite sides of sample (see Fig. 1). Unlike SORS it is not able to provide the signatures of individual layers within the sample, instead it provides volumetric information on the entire volume of the sample. This is beneficial in situations where one is, for example, searching for a specific signal at unknown location in a large volume of sample such as in breast cancer diagnosis. Vardaki *et al.*[15] recently studied the dependence of TRS signals on sample location in phantoms exhibiting the optical properties of biological tissues with relevance to breast cancer and prostate cancer diagnosis. This extended on earlier studies of pharmaceutical samples of similar nature, but with markedly different optical properties. The key observation of this study was that the weakest signal is detected from a given object (*e.g.* cancer lesion) within the centre of the volume, in contrast with findings of layered pharmaceutical tablets where the highest signal is observable at the centre of the tablet. This difference is ascribed to the extended nature of the layers used with pharmaceutical tablets whereas in the case of sampling calcifications in breast tissue a more spatially confined target is present. In the worst case scenario modelling breast and prostate tissues, around 50% lower signals were observed centrally than the maximum signal near the surface. Ghita *et al.* investigated the optimum excitation wavelength for probing large volumes in tissues using TRS.[16] The study included tissue absorption and fluorescence effects. It concluded that the optimum laser excitation wavelength range for detecting hydroxyapatite $\sim$960 cm^{-1} with highest sensitivity is around 800 nm.

Raman tomography

Schulmerich *et al.*[17] showed that the spatial offset Raman concept can also be used to retrieve both spatial and chemical information, facilitating a chemically specific tomographic capability with Raman spectroscopy. The researchers demonstrated tomographic imaging of phantoms and canine limb including skin and tissue up to thicknesses of 45 mm.[18] The technique was further developed by Srinivasan *et al.*[19] by introducing image-guided Raman spectroscopy using X-ray computed tomography images of the tissue in conjunction to guide the numerical recovery of Raman images.[20] Further optimisation of this technique was performed by Demers *et al.*[21]

Micro-SORS

Recently the SORS concept has also been combined with microscopy to resolve very thin, highly turbid layers, such as those present with paints in paintings.[22] The technique was demonstrated to be beneficial to analysing the objects of art[23] as well as stratified polymers, paper and wheat seeds.[24] Its penetration depth was estimated using Monte Carlo simulations to be an order or two of magnitude larger than that of conventional confocal Raman microscopy.[25] The concept is anticipated to have a number of biomedical applications such as probing through skin or other interfaces although these are still in formative stages.

SESORS

A powerful modality of SORS combining the deep penetration properties of SORS with high sensitivity and specificity of surface enhanced Raman spectroscopy (SERS) was demonstrated by Stone *et al.*[26] The method, known as SESORS, facilitates the

extension of applicability of SERS to subsurface analysis of medical tissues and other diffusely scattering media. Although it requires the introduction of SERS nanoparticles or SERS substrate into the sample its subsequent readout can be fully non-invasive. The reporter labelled and functionalised nanoparticles can facilitate highly specific identification and localisation of the presence of a particular disease specific cellular expression. A demonstration of SESORS for non-invasive multiplexed imaging of buried structures deep within tissue, with high chemical specificity, was further shown by Stone *et al.*[27] This study evidenced that SESORS signals can be recovered non-invasively from depths of up to 45–50 mm in biological tissues. As a non-label-free variant of SORS the medical applications of SESORS *in vivo* are hampered by the potential toxicity issues associated with the introduction of SERS nanoparticles into living body that to date have not been fully addressed. However these issues can be mitigated to large extent by confining the SERS nanoparticles to a substrate (*e.g.* 'SERS subcutaneous implant').

Applications

A number of potential medical uses of deep Raman spectroscopy are currently under investigation in several laboratories. Given the relative novelty of the non-invasive deep Raman techniques these are in their very early stages of development, still several years away from clinical applications. Nevertheless the first results are promising indicating the potential extent of these methods to address key societal challenges if the developments are successfully completed. A few representative examples of these emerging medical applications are discussed below.

Non-invasive diagnosis of breast cancer

Both the SORS and transmission Raman spectroscopy concepts are potentially amenable to non-invasive detection and characterisation of cancer lesions in breast tissue *in vivo*. Breast cancer is a prevalent condition, for example, affecting around 1 in 8 women during their lifetime in the UK with annual incidence amounting to around 48 000 women.[28] To enable early diagnosis, which offers more conservative treatments and better patient outcomes, the UK's National Health Service (NHS) runs a mammographic screening programme involving women over 50 years of age. Since its initiation there has been a 17.5% decrease in deaths from breast cancer for women aged 50–70 years (1996–2005).[29] Despite these successes the screening suffers from several limitations; (i) the mammography is only effective with female breasts which are less dense and (ii) the identification of a suspect lesion does not convey information about whether the lesion is benign or malignant. To establish the malignancy status a needle biopsy is typically carried out. Approximately 4.4% (2008/9) of 2.1 million women screened were referred for further tests and out of the referred ones only 18% were found to have malignancies.[30] As such 82% of women referred from screening in 2008/9 had investigations including excisional biopsy – with all the associated risks (from increased radiation dose to infection), costs to the NHS and inevitable psychological stress to the patient and their close relatives and friends – when they had no malignancies present.

The provision of a safe, rapid non-invasive method in conjunction with mammography could avoid the biopsy step and associated adverse impact on patient and NHS. The first seeds for this potential were laid by Haka *et al.*[31] who recognised that the chemical content of micro-calcifications associated with benign and malignant calcifications are significantly different and that this difference is reflected also in Raman spectra. The study indicated that microcalcifications can be divided into two types: (i) Type I consisting of calcium oxalate dihydrate, and (ii) Type II consisting of calcium phosphates, mainly calcium hydroxyapatite. Calcium oxalate crystals (Type I) are mainly found in benign ductal cysts and rarely found in carcinoma,[32] whereas calcium hydroxyapatite deposits (Type II) are present in proliferative lesions, which can include lesions of both benign and malignant pathology and these can be further subdivided into benign and malignant classes depending on their carbonate contents.[31] Baker *et al.*[33] further showed using Fourier transform infrared imaging that for Type II calcifications the chemical composition is not only specific to benign and malignant calcifications but it follows a continuum, from benign through the full range of ductal carcinomas *in situ* and invasive cancers. This is reflected most profoundly in the reduction of carbonate ion substitutions within calcium hydroxyapatite crystal lattice as the neighbouring tissue is transformed from benign to invasive disease.

The above implies that the observation of Type I calcifications signals the presence of a benign lesion. The detection of Type II calcifications represents an ambiguous situation as these are found both with benign and malignant lesions. However, these can be further differentiated into benign and malignant lesions by their carbonate content. Such chemical characterisation would not be possible reliably by mammography.

The TRS research reached the clinically relevant concentration range with a penetration depth of 20 mm in porcine tissue (see Fig. 2).[34] This is about 2.5-times lower that the clinical penetration depth ($\sim$50 mm) for wider screening use.[35] It is also worth noting that the depth of 20 mm is approximately two orders of magnitude higher than possible with conventional Raman spectroscopy approaches. Further increase of penetration depth is however achievable by further enhancing the quality of the detected Raman signal by boosting its intensity. This is due the fact that for deep Raman technique the detection sensitivity is ultimately determined by the quality of Raman signal retrieved and this mostly depends on its intensity. The intensity of the detected Raman signal can be boosted by increasing the laser power incident on tissue although potential for photo-damage is possible at high power densities and associated safety illumination levels pose stringent limits here. Nevertheless these can be circumvented to a great degree using extended illumination areas (*e.g.* possible with inverse SORS and TRS geometries). The signal levels can also be boosted by enhancing Raman collection efficiency of spectrographs (etendue). This can be accomplished by further opening spectrograph slits permitted by higher dispersion gratings (consequently resulting also in narrower spectral ranges) or by purposely degrading spectral resolution in applications where the spectral resolution is not a critical parameter (*e.g.* when distinguishing calcium oxalate

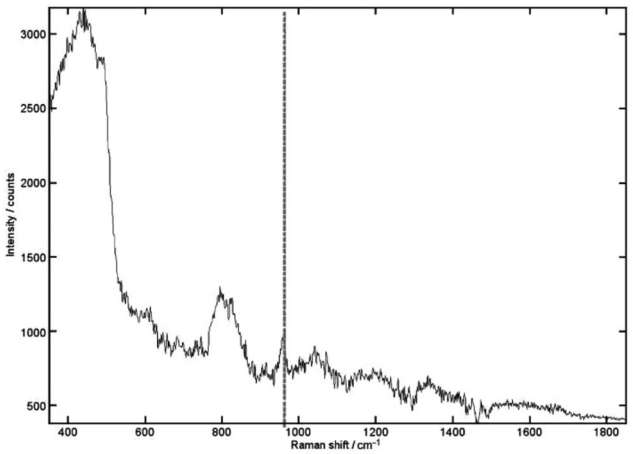

Fig. 2 The recovered signal achieved for 0.125% (relative volume) of HAP buried within 20 mm of porcine tissue. The 962 cm^{-1} peak is still clearly recognizable. Acquisition times were 5 s with 10 accumulations. Vertical line, HAP peak.[34] (Reprinted with permission from N. Stone and P. Matousek, *Cancer Res.*, 2008, **68**, 4424 with permission of the American Association for Cancer Research, Inc.)

from calcium hydroxyapatite where marked bands are well separated from each other and other main components of tissue). In the case of breast cancer diagnosis these above measures along with the enhanced data processing methods using advanced multivariate analysis tools promise to more than double the existing penetration depths.[34,36]

As mentioned above in situations where the separation of Type II calcifications into subclasses is required the carbonate content could be evaluated by deriving directly the ratio of phosphate and carbonate Raman bands at $\sim$960 cm^{-1} and $\sim$1070 cm^{-1}, respectively. This can however be challenging in subsurface analysis as the carbonate Raman band at $\sim$1070 cm^{-1} is relatively weak and overlapped with Raman collagen bands of tissue. Kerssens *et al.*[37] showed an alternative way of characterising the carbonate content, by direct monitoring of the position and bandwidth of the intense $\sim$960 cm^{-1} phosphate Raman band alone. This provides information on the carbonate content as this band's parameters are sensitive to carbonate inclusions in the lattice.

Determination of cancer margins

Another important unaddressed clinical need is the determination of cancer margins during cancer removal surgery. It is important to remove enough of tissue to ensure that no cancerous cells remain but at the same time the surgeon needs to strive for minimising the amount of normal tissue removed for medical or aesthetic reasons. In this area, Keller *et al.*[38] performed a conceptual study applying SORS to the identification of soft tissue lesions at depths of several mm's. Further improvement of the SORS geometry in this application enabled the sample characterisation up to depths of 2 mm.[39] A probabilistic scheme was used to classify the composite spectra as 'negative' or 'positive' margins. The discrimination achieved had 95% sensitivity and 100% specificity, when tested using a leave-one-out methodology. Although a number of questions about its efficacy warrant further investigations this work demonstrates that SORS of soft tissues holds considerable promise for biomedical applications.

Bone disease diagnosis

Conventional Raman spectroscopy has been used in the analysis of bone matrix *ex vivo* very widely.[40] The advent of SORS opened new avenues in the area of non-invasive characterisation of bone through soft tissue *in vivo*.[40–42] In this area the clinical need stems from considerable inefficacy of existing methods. For example the diagnosis of osteoporosis is traditionally performed by Dual-energy X-ray Absorptiometry (DXA) which has accuracy for predicting osteoporotic fractures of only 60–70%. This is, in part, due to its inability to sense the organic component of bone, predominantly consisting of collagen. As this constituent plays a crucial role in providing bone mechanical properties (*e.g.* toughness) this is considered a major deficiency of the method. In contrast SORS is capable of providing information on both the key components of bone, organic and inorganic. Therefore its use in this context promises to deliver major improvements in diagnostic accuracy of various bone conditions.

The application of SORS for transcutaneously characterising bones was first demonstrated by Schulmerich *et al.*[43] The researchers attained depths of several millimetres through soft tissue in animal and human cadavers. The technique was then rapidly advanced expanding the penetration depths to above 4 mm.[42,44] Okagbare *et al.* developed a multiple-fibre optic Raman probe allowing the collection of Raman spectra from multiple points around a limb to increase accuracy of recovered bone spectra to enable the monitoring of more subtle changes in composition.[45] This was demonstrated with rat tibia phantoms in which the bone had carbonated hydroxyapatite with different carbonate concentrations.

More recently, the research in this area had progressed to include *in vivo* trials on humans within the operating theatre enabling researchers to perform a direct comparison, for the first time, of *in vivo* transcutaneous data with those obtained from *in vivo* exposed bone in surgery on the same patient.[46] Preliminary data demonstrate that good correspondence between the exposed data and transcutaneous data can be achieved.

Transcutaneous Raman is also under development for early detection of burn induced heterotopic ossification (HO) of soft tissue,[47] a condition associated with major burn injuries and blast traumas. The potential of this approach was demonstrated on mice following a burn injury (see Fig. 3). Raman data showed significantly increased bone mineral signalling in the tenotomy (surgical procedure) compared to control leg at 5 days post injury, with the difference increasing over time. In contrast, micro CT did not demonstrate heterotopic bone until three weeks post injury. Changes in bone mineral and matrix composition of the new bone were also evidenced in the Raman spectra which could facilitate early identification of HO and allow more timely therapy decisions for HO patients.

Recently, Buckley *et al* applied inverse SORS[10,11] to noninvasive diagnosis of *osteogenesis imperfecta* ('brittle bone') condition *in vivo*.[48]

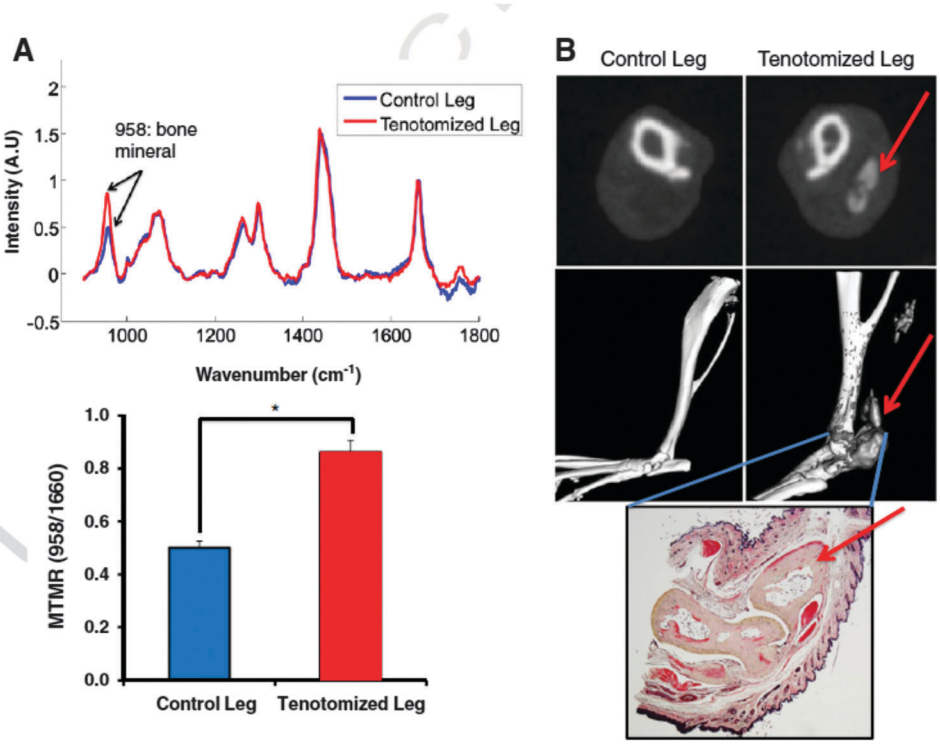

Fig. 3 Raman spectroscopy and cross sectional Micro CT of Achilles tenotomy model on non-injured and on tenotomized leg at 3 months after injury and burn. (A) (top) Raman spectra of tenotomized leg (red) and non-tenotomized control leg (blue) of a burn mouse that had known HO growth. Spectra are normalized to the protein matrix and collagen band at 1600 cm^{-1} and superimposed to show differences in bone mineral signal at 958 cm^{-1} (bottom) mineral to matrix ratio from Raman spectra demonstrates increased mineral content in the tenotomized leg (*, pb 0.05). (B) Micro CT confirmation of HO growth in the tenotomized leg seen in representative CT slices (top) and 3D reconstructions (middle). Red arrows indicate HO formation. Gray areas in the reconstructed image indicate ectopic bone. Histologic verification of ectopic bone growth with pentachrome stain (bottom) showing bone as pale yellow. Red arrow indicates HO formation. (For interpretation of the references to colour in this figure legend, the reader is referred to the web version of this article.)[47] (Reprinted from J. R. Peterson, P. I. Okagbare, S. De La Rosa, K. E. Cilwa, J. E. Perosky, O. N. Eboda, A. Donneys, G. L. Su, S. R. Buchman, P. S. Cederna, S. C. Wang, K. M. Kozloff, M. D. Morris, B. Levi, 'Early detection of burn induced heterotopic ossification using transcutaneous Raman spectroscopy', *Bone*, **54**, 28–34, Copyright (2013), with permission from Elsevier.)

The study succeeded in detecting the presence of this condition within a single patient. The obtained spectra were also consistent with Raman spectra obtained *ex vivo* from the same patient (see Fig. 4). Although the study is only the first step towards delivering a diagnostic method it outlines the potential of SORS in this area. Although it should be noted that specifically in the case of *osteogenesis imperfecta*, which is genetic condition, effective DNA screening methods also exist although in the UK, for example, these are not yet in routine use.

In the area of the diagnosis of osteoporotic conditions by SORS progress has also been recently made. Buckley *et al.*[49] demonstrated the potential of SORS in this area building on earlier advances by Morris' group.[42] Buckley's study showed that on average, bone fragments from the necks of fractured femora measured *ex vivo* are more mineralised (by 5–10%) than (cadaveric) non-fractured controls, but the mineralisation distributions of the two cohorts are largely overlapped. SORS *in vivo* measurements indicated a potential of the presence of similar differences but these were as yet statistically underpowered. The study also identified methodological developments which could be implemented to improve the statistical significance of future experiments that may eventually lead to more sensitive prediction of fragility fractures *in vivo*.

It should, however, be noted that, in general, this is a difficult area to penetrate due to the widespread of DXA technique, despite DXA existing limitations, and only considerable outperformance of DXA by deep Raman methods would be expected lead to the change of medical practice. Initially, the deep Raman methods are likely to be used as complementary tools to the existing methods rather than replacing them outright.

Glucose detection

Kong *et al.* has demonstrated a potential of TRS to directly monitor glucose levels noninvasively using transmission Raman spectroscopy without recourse to labelling.[50] This was accomplished using a novel high-collection efficiency optical system based on non-imaging optics (compound hyperbolic concentrator) and incorporated within a portable system. Raman spectra of 18 volunteers were acquired and the glucose levels were sampled *in vivo* through thenar skin fold in human subjects and predicted successfully. The use of the SESORS techniques has been demonstrated to be potentially very promising too. However, in this application a SERS implant needs to be inserted under skin but subsequent readout is non-invasive. Given the considerably higher strength of SERS signals compared with normal Raman

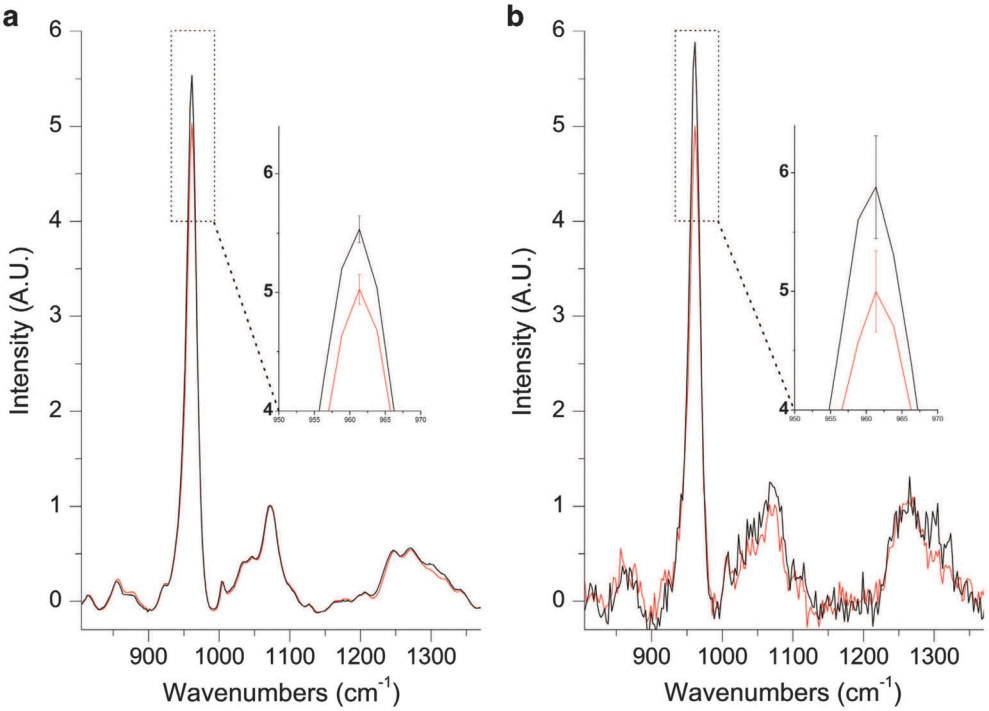

Fig. 4 (a) A Raman spectrum of excised OI bone (black) and excised control bone (red). The inset shows mean ± s.d. (b) A spatially offset Raman spectrum retrieved noninvasively through the skin of the same OI patient (black) and a spatially offset Raman spectrum retrieved noninvasively through the skin of an age-matched control (red). The inset shows mean ± s.d.[48] (Reprinted with permission from K. Buckley, J. G. Kerns, P. D. Gikas, H. L. Birch, J. Vinton, R. Keen, A. W. Parker, P. Matousek, A. E. Goodship, *IBMS BoneKEy*, 2014, **11**, 602 with permission of the Nature Publishing Group.)

this technology promises to be deployable with much cheaper readout units. Yuen *et al.* has demonstrated this application in rats *in vivo*.[51] They fabricated a SERS substrate consisting of silver film over nanosphere surface functionalised with a mixed self-assembled monolayer and implanted it subcutaneously into a rat. The glucose levels were successfully measured in this study using SORS *in vivo* through soft skin tissue at clinically relevant levels over a 17 day period.[52]

Although it should be pointed out that this is a very challenging area under intense focus of many groups worldwide utilising a wide range of techniques. As such Raman techniques will face tough competition in the market place and their ultimate success will depend on social economic benefits they would bring as well as the robustness and accuracy of these.

Non-invasive probing through skull

There are numerous other biomedical applications also under consideration and development. One such a new avenue is the non-invasive probing of skull using SESORS for the detection of bioanalytes directly in brain tissue. The first proof-of-concept study in this direction has been carried out by Sharma *et al.*[53] demonstrating the ability of SESORS to measure spectra through various thicknesses of bone (3–8 mm). The study also showed that diluted nanotag samples (comparable to 2×10^{12} particles) and their concentration could be detected through the bone (see Fig. 5). It is anticipated that these through-bone SESORS measurements will enable real-time, non-invasive spectroscopic measurement of neurochemicals through the skull, as well as other biomedical applications in related areas. Although it should be noted that injecting nanoparticles into human brain is an untested and highly controversial area. It is expected that such techniques are likely to be first adopted with rodents leaving the diagnosis of human brain a longer term prospect subject to addressing satisfactorily all pertinent safety issues first.

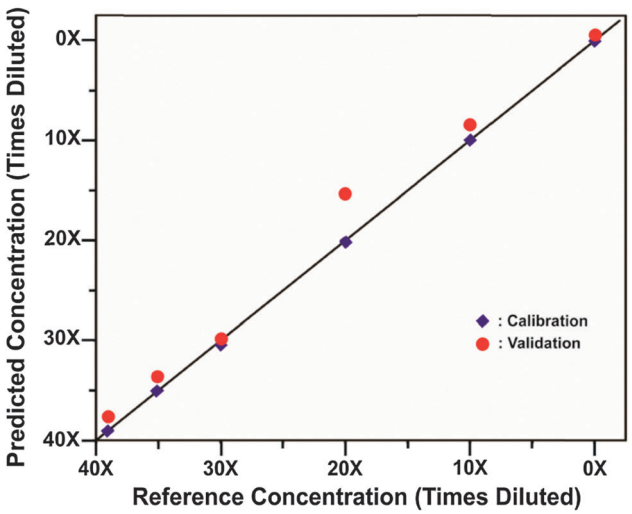

Fig. 5 Calibration and validation data sets of SESORS quantitative measurements of BPE functionalized SERS nanotags through bone.[53] (Reprinted with permission from B. Sharma, K. Ma, M. R. Glucksberg, R. P. Van Duyne, *J. Am. Chem. Soc.*, 2013, **135**, 17290 Copyright (2013) American Chemical Society.)

Conclusions

The recent progress in the area of deep Raman spectroscopy facilitated by the advent of SORS and transmission Raman spectroscopy and their use in biomedical applications paves the way for a range of novel applications in numerous medical fields. These include the diagnosis of bone disease and breast cancer, determination of cancer margins, chemically specific tomographic imaging of tissues, the detection of glucose levels and monitoring the brain conditions through skull. In addition it is likely the use of multiplexed SESORS could lead to advances in tumour specific treatment selection and monitoring in real-time.

Acknowledgements

Funding from EPSRC (EP/K020374/) is gratefully acknowledged.

References

1 P. Matousek, I. P. Clark, E. R. C. Draper, M. D. Morris, A. E. Goodship, N. Everall, M. Towrie, W. F. Finney and A. W. Parker, *Appl. Spectrosc.*, 2005, **59**, 393.
2 *Emerging Raman Applications and Techniques in Biomedical and Pharmaceutical Fields*, ed. P. Matousek and M. D. Morris, Springer, Heidelberg, 2010.
3 T. J. Pfefer, K. T. Schomacker, M. N. Ediger and N. S. Nishioka, *Appl. Opt.*, 2002, **41**, 4712.
4 N. Everall, T. Hahn, P. Matousek, A. W. Parker and M. Towrie, *Appl. Spectrosc.*, 2004, **58**, 591.
5 E. Widjaja, N. J. Crane, T. C. Chen, M. D. Morris, M. A. Ignelzi and B. R. McCreadie, *Appl. Spectrosc.*, 2003, **57**, 1353.
6 J. R. Maher, J. A. Inzana, H. A. Awad and A. J. Berger, *J. Biomed. Opt.*, 2013, **18**, 077001.
7 H. M. Kim, H. S. Park, Y. Cho, S. M. Jin, K. T. Lee, Y. M. Jung and Y. D. Suh, *J. Mol. Struct.*, 2014, **1069**, 223.
8 P. Gemperline, *Practical Guide to Chemometrics*, Taylor & Francis, Boca Raton, 2006.
9 A. M. Smith, M. C. Mancini and S. Nie, *Nat. Nanotechnol.*, 2009, **4**, 710.
10 P. Matousek, *Appl. Spectrosc.*, 2006, **60**, 1341.
11 M. V. Schulmerich, K. A. Dooley, M. D. Morris, T. M. Vanasse and S. A. Goldstein, *J. Biomed. Opt.*, 2006, **11**, 060502.
12 J. R. Maher and A. J. Berger, *Appl. Spectrosc.*, 2010, **64**, 61.
13 M. Bloomfield, P. W. Loeffen and P. Matousek, *Proc. SPIE*, 2010, **7838**, 783808.
14 B. Schrader and G. Bergmann, *Z. Anal. Chem.*, 1967, **225**, 230.
15 M. Z. Vardaki, B. Gardner, N. Stone and P. Matousek, *Analyst*, 2015, **140**, 5112–5119.
16 A. Ghita, P. Matousek and N. Stone, Exploration of Effect of Laser Excitation Wavelength on Signal Recovery with Deep Tissue Transmission Raman Spectroscopy, in preparation.
17 M. V. Schulmerich, W. F. Finney, R. A. Fredricks and M. D. Morris, *Appl. Spectrosc.*, 2006, **60**, 109.
18 M. V. Schulmerich, J. H. Cole, K. A. Dooley, M. D. Morris, J. M. Kreider, S. A. Goldstein, S. Srinivasan and B. W. Pogue, *J. Biomed. Opt.*, 2008, **13**, 020506.
19 S. Srinivasan, M. Schulmerich, J. H. Cole, K. A. Dooley, J. M. Kreider, B. W. Pogue, M. D. Morris and S. A. Goldstein, *Opt. Express*, 2008, **16**, 12190.
20 C. M. Carpenter, B. W. Pogue, S. Jiang, H. Dehghani, X. Wang, K. D. Paulsen, W. A. Wells, J. Forero, C. Kogel, J. B. Weaver, S. P. Poplack and P. A. Kaufman, *Opt. Lett.*, 2007, **32**, 933.
21 J. L. H. Demers, S. C. Davis, B. W. Pogue and M. D. Morris, *Biomed. Opt. Express*, 2012, **3**, 2299.
22 C. Conti, C. Colombo, M. Realini, G. Zerbi and P. Matousek, *Appl. Spectrosc.*, 2014, **68**, 686.
23 C. Conti, M. Realini, C. Colombo and P. Matousek, *J. Raman Spectrosc.*, 2015, **46**, 476–482.
24 C. Conti, M. Realini, C. Colombo, K. Sowoidnich, N. K. Afseth, M. Bertasa, A. Botteon and P. Matousek, *Anal. Chem.*, 2015, **87**, 5810–5815.
25 P. Matousek, C. Conti, C. Colombo and M. Realini, Monte Carlo Simulations of Subsurface Analysis of Painted Layers in Micro-Scale Spatially Offset Raman Spectroscopy, *Appl. Spectrosc.*, 2015, **69**, 1091–1095.
26 N. Stone, K. Faulds, D. Graham and P. Matousek, *Anal. Chem.*, 2010, **82**, 3969.
27 N. Stone, M. Kerssens, G. R. Lloyd, K. Faulds, D. Graham and P. Matousek, *Chem. Sci.*, 2011, **2**, 776.
28 ONS. Cancer statistics registrations: Registrations of cancer diagnosed in 2008, England. MB1 no 38. London: National Statistics, 2011.
29 www.ic.nhs.uk/pubs/brstscreen0809.
30 www.cancerscreening.nhs.uk.
31 A. S. Haka, K. E. Shafer-Peltier, M. Fitzmaurice, J. Crowe, R. R. Dasari and M. S. Feld, *Cancer Res.*, 2002, **62**, 5375.
32 M. J. Radi, *Arch. Pathol. Lab. Med.*, 1989, **113**, 1367.
33 R. Baker, K. D. Rogers, N. Shepherd and N. Stone, *Br. J. Cancer*, 2010, **103**, 1034.
34 N. Stone and P. Matousek, *Cancer Res.*, 2008, **68**, 4424.
35 F. Sardanelli, F. Zandrino, A. Imperiale, E. Bonaldo, M. G. Quartini and N. Cogorno, *Radiology*, 2000, **217**, 576.
36 P. Matousek and N. Stone, *J. Biomed. Opt.*, 2007, **12**, 024008.
37 M. M. Kerssens, P. Matousek, K. Rogers and N. Stone, *Analyst*, 2010, **135**, 3156.
38 M. D. Keller, S. K. Majumder and A. Mahadevan-Jansen, *Opt. Lett.*, 2009, **34**, 926.
39 M. D. Keller, E. Vargis, N. de Matos Granja, R. H. Wilson, M.-A. Mycek, M. C. Kelley and A. Mahadevan-Jansen, *J. Biomed. Opt.*, 2011, **16**, 077006.
40 A. Carden and M. D. Morris, *J. Biomed. Opt.*, 2000, **5**, 259.
41 E. R. C. Draper, M. D. Morris, N. P. Camacho, P. Matousek, M. Towrie, A. W. Parker and A. E. Goodship, *J. Bone Miner. Res.*, 2005, **20**, 1968.
42 B. R. McCreadie, M. D. Morris, T. Chen, D. S. Rao, W. F. Finney, E. Widjaja and S. A. Goldstein, *Bone*, 2006, **39**, 1190.
43 M. V. Schulmerich, W. F. Finney, V. Popescu, M. D. Morris, T. M. Vanasse and S. A. Goldstein, *Proc. SPIE*, 2006, **6093**, 60930O.
44 G. S. Mandair, F. W. L. Esmonde-White, M. P. Akhter, A. M. Swift, J. Kreider, S. A. Goldstein, R. R. Recker and M. D. Morris, *Proc. SPIE*, 2010, **7548**, 754846.

45 P. I. Okagbare, F. W. L. Esmonde-White, S. A. Goldstein and M. D. Morris, *Analyst*, 2010, **135**, 3142.
46 F. W. L. Esmonde-White and M. D. Morris, *Proc. SPIE*, 2013, **8565**, 85656K.
47 J. R. Peterson, P. I. Okagbare, S. De La Rosa, K. E. Cilwa, J. E. Perosky, O. N. Eboda, A. Donneys, G. L. Su, S. R. Buchman, P. S. Cederna, S. C. Wang, K. M. Kozloff, M. D. Morris and B. Levi, *Bone*, 2013, **54**, 28.
48 K. Buckley, J. G. Kerns, P. D. Gikas, H. L. Birch, J. Vinton, R. Keen, A. W. Parker, P. Matousek and A. E. Goodship, *IBMS BoneKEy*, 2014, **11**, 602.
49 K. Buckley, J. G. Kerns, J. Vinton, P. D. Gikas, C. Smith, A. W. Parker, P. Matousek and A. E. Goodship, *J. Raman Spectrosc.*, 2015, **46**, 610–618.
50 C. R. Kong, I. Barman, N. C. Dingari, J. W. Kang, L. Galindo, R. R. Dasari and M. S. Feld, *AIP Adv.*, 2011, **1**, 032175.
51 J. M. Yuen, N. C. Shah, J. T. Walsh, M. R. Glucksberg and R. P. Van Duyne, *Anal. Chem.*, 2010, **82**, 8382.
52 K. Ma, J. M. Yuen, N. C. Shah, J. T. Walsh, M. R. Glucksberg and R. P. Van Duyne, *Anal. Chem.*, 2011, **83**, 9146.
53 B. Sharma, K. Ma, M. R. Glucksberg and R. P. Van Duyne, *J. Am. Chem. Soc.*, 2013, **135**, 17290.

